ACS OMEGA

Open Access

This article is licensed under CC-BY-NC-ND 4.0

http://pubs.acs.org/journal/acsodf

Article

Silencing of LncRNA XIST Suppressed Tumor Growth and Metastasis in Papillary Thyroid Carcinoma by Modulating miR-204/FN1 Axis

Jie Qiu, Maolin Sun, Zuorong Qin, Mingbo Liu, and Wenwei Zhang*

Cite This: *ACS Omega* 2025, 10, 19643−19654

Read Online

ACCESS | Metrics & More | Article Recommendations

ABSTRACT: Papillary thyroid carcinoma (PTC) is a prevalent endocrine malignancy with a high incidence rate of regional lymph node metastasis. Dysregulation of lncRNA XIST has been observed in various malignancies. This study aims to elucidate the molecular mechanism of lncRNA XIST in PTC metastasis. Quantitative real-time PCR assays were conducted to detect the expression levels of XIST, FN1, and miR-204−5p in PTC tissues. Meanwhile, loss-of-function assays were employed to evaluate the oncogenic roles of XIST in PTC cell lines. Our results revealed significant overexpression of XIST and FN1 in PTC tissues and cell lines, accompanied by decreased levels of miR-204−5p ($p < 0.05$). Knockdown of XIST or FN1 inhibited cellular proliferation, metastasis, and invasion in PTC cells, upregulated E-cadherin, and downregulated N-cadherin and Vimentin. Furthermore, we demonstrated that XIST regulates FN1 expression by competitively binding to miR-204−5p. MiRNA inhibitor rescue assays confirmed the pivotal role of the XIST/miR-204/FN1 axis in PTC metastasis and invasion. Our study underscores the oncogenic role of XIST in PTC by acting as a sponge for miR-204, regulating FN1 expression. These findings hold promise for advancing our understanding of thyroid cancer and developing potential therapeutic and diagnostic targets for PTC.

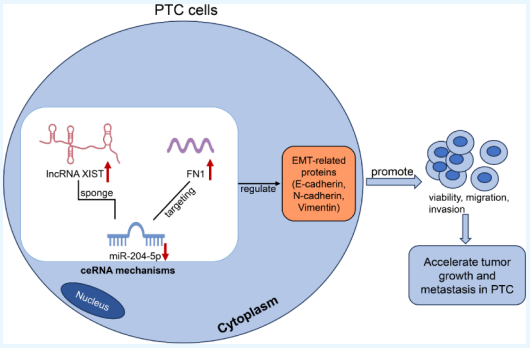

INTRODUCTION

Papillary thyroid carcinoma (PTC) constitutes 90% of diagnosed cases with a favorable prognosis, and approximately 30−40% cases metastasize to regional lymph nodes, resulting in substantial reduction in survival rates.[1] The mainstay treatment for patients with differentiated thyroid cancer involves thyroidectomy, radioiodine therapy, and thyrotrophic suppression. While this regimen can cure most patients, a subset may still develop regional recurrence or distant metastasis, rendering radioactive iodine treatment ineffective.[2,3] Despite therapeutic advancements, challenges persist regarding optimal patient risk stratification and the emergence of unresponsive and acquired resistance to approved therapies. Therefore, the identification of reliable diagnostic markers and potential targets for early detection and treatment of PTC remains of principle clinical significance.

Long noncoding RNA (lncRNA) XIST is a 17-kb lncRNA transcript associated with X chromosome inactivation in mammals, facilitating dosage compensation between the sexes for X-linked genes.[4] XIST spans the X chromosome in cis, orchestrating chromosome-wide gene silencing.[5] Mechanistically, XIST achieves transcriptional repression via direct interaction with transcriptional repressors SHARP/SMRT to activate HDAC3, deacetylating histones to preclude RNA-Pol II across the X chromosome.[6] Dysregulation of lncRNA-XIST has been extensively documented across various cancer types, with numerous studies highlighting its pathogenic role in digestive system tumors,[7−9] respiratory system tumors,[10−12] and nervous system tumors,[13−15] gynecolgical tumors,[16,17] promoting tumor growth, metastasis, and chemotherapy resistance. Notably, XIST also assumes a tumor-suppressive role in certain cancers like hematologic malignancy,[18] renal carcinoma,[19] and ovarian cancer.[20] In PTC, lncRNA-XIST was reported to promote migration and invasion via tarting miR-141[21] or modulating miR-101−3p/CLDN1 axis[22] and miR-330−3p/PDE5A axis.[23] Nevertheless, the specific role of lncRNA-XIST in PTC remains elusive.

MiR-204 has emerged as a crucial tumor suppressor in various cancers, including PTC, demonstrating inhibitory effects on proliferation, metastasis, cell cycle progression, and apoptosis induction in cellular experiments.[24,25] MiR-204−5p can directly target multiple downstream genes, such as AP1S2[26] and HMGA2,[27] affecting epithelial mesenchymal transition (EMT) and invasion processes in PTC. Further-

Received: January 14, 2025
Revised: April 27, 2025
Accepted: April 29, 2025
Published: May 6, 2025

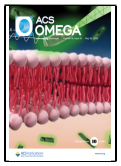

© 2025 The Authors. Published by American Chemical Society

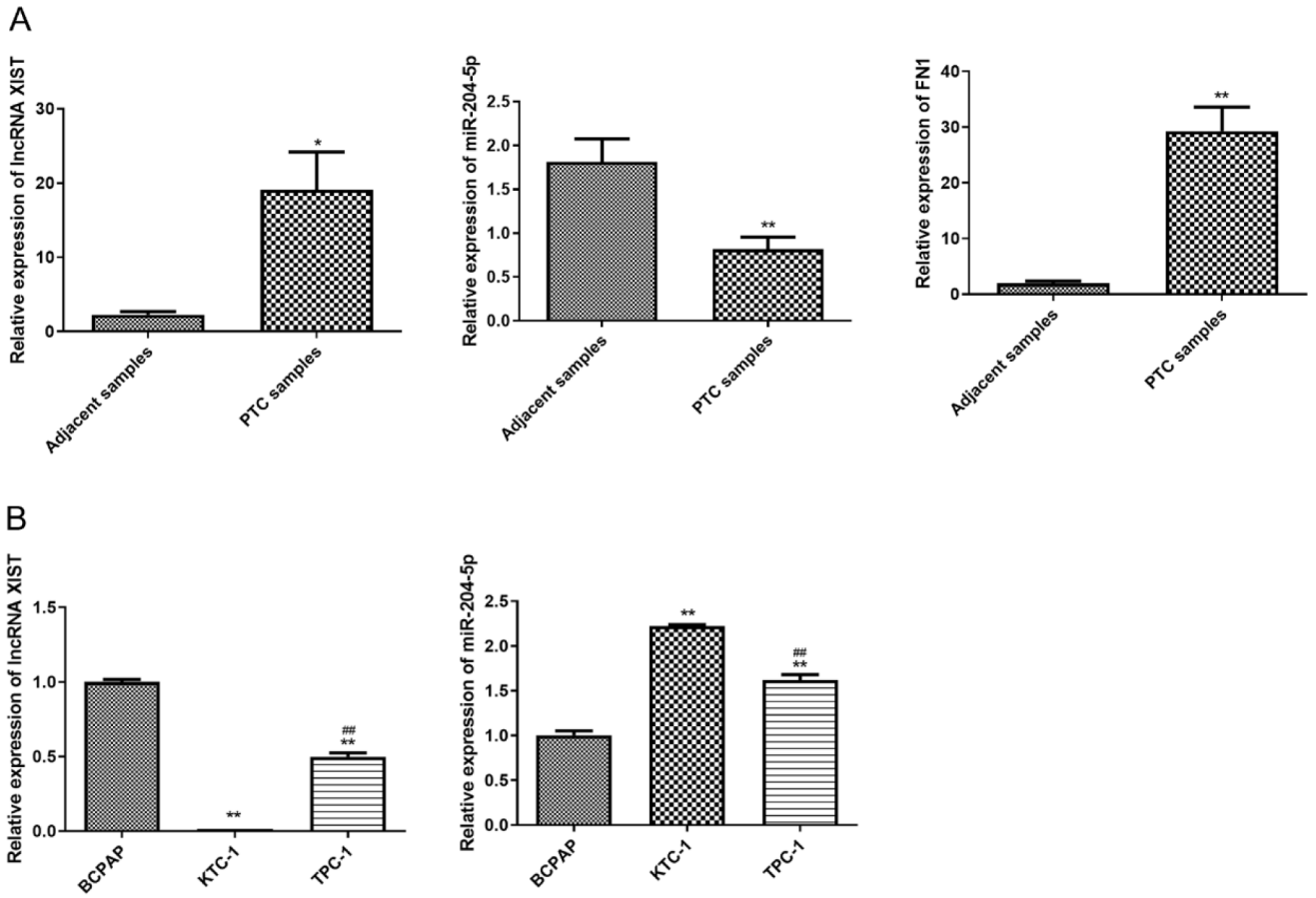

Figure 1. qRT-PCR analysis revealed that expression of lncRNA XIST, FN1, and miR-204−5p in PTC samples (n = 20) (A) and cell lines (B). * p < 0.05, ** p < 0.01 compared with adjacent samples or BCPAP cells; ##, p < 0.01 compared with KTC-1 cells.

more, miR-204−3p, in combination with other miRNAs, has exhibited potential as refined diagnostic markers for the thyroid neoplasia spectrum.[28] Emerging research underscores the role of lncRNA XIST as sponge of miR-204, influencing its expression through competing endogenous RNA (ceRNA) activity in glioma,[29] retinoblastoma,[30] and endothelial cell injury.[31] We hypothesized that lncRNAs-XIST might act as sponges for miR-204 and consequently influence downstream target gene expression.

In our previous research, miR-204 potential targets were predicted by online platform miRwalk, and protein of FN1 was selected.[32] Fibronectin or FN1 serves as a key component of ECM and exerted diverse physiological functions in embryogenesis, wound healing, hemostasis, cell adhesion and migration.[33−35] Consisting of two similar yet distinct 220 and 250 kDa monomers connected by two disulfide bridges at the C terminus, FN1 is characterized by repeating modules (FNI, FNII, and FNIII) within each monomer. These modules harbor binding sites for extracellular molecules like integrin, collagen, and heparin.[36] Plasma FN1 (pFN) and cellular FN1 (cFN) are two distinct forms. The former is consistently synthesized by hepatocytes, while cFN is produced by various cell types, including chondrocytes, fibroblasts, and endothelial cells. Extracellular FN1 has been extensively studied for its pivotal role in tumorigenesis, metastasis, and chemoresistance.[37,38] However, the biological roles of FN1 in PTC remain to be enunciated. This study aims to present a novel theoretical perspective on the lncRNA-XIST/miR-204−5p/FN1 axis underlying metastasis in PTC progression. Our research lays the foundation for innovative data and methodologies targeted at clinically addressing PTC treatment.

RESULTS

Expression Levels of lncRNA XIST and FN1 in PTC Tissue and Cell Lines. Previous researches have demonstrated that lncRNA-XIST can function as sponge of miR-204 to regulate downstream mRNAs via sponging miRNAs.[29−31] In addition, we found FN1 is one of the target genes of miR-204.[32] Therefore, we hypothesized that lncRNA XIST might act as sponges for miR-204 and consequently influence the gene expression of FN1. The expression of lncRNA XIST, miR-204−5p, and FN1 were detected in PTC samples and adjacent normal samples first using qRT-PCR analysis. It was found that compared with the adjacent normal samples, the expression levels of lncRNA XIST and FN1 were significantly upregulated in tumor tissue samples, while the miR-204−5p level was significantly reduced in the PTC tissues (Figure 1A, p < 0.05).

Meanwhile, the expression level of XIST and miR-204−5p were measured in three PTC cell lines, and the results showed the BCPAP cells had the highest expression level of XIST and the lowest expression level of miR-204−5p compared to the KTC-1 and TPC-1 cells (Figure 1B, p < 0.05). Therefore, we selected BCPAP cells to conduct the following experiments.

Further, we used bioinformatics analysis to investigate the correlations between XIST, miR-204−5p, and FN1 levels with clinical parameters. It was shown that the XIST expression was significantly associated with age, gender, and pathologic-T

https://doi.org/10.1021/acsomega.5c00390
ACS Omega 2025, 10, 19643−19654

Table 1. Correlations between the XIST Expression and Clinical Information

Characteristic total cases	N of case 500	XIST expression		χ2	P value
		Low (N = 250)	**High** (N = 250)		
		Age (years)			
≤60	387	180	207	7.729	5.43×10^{-03}
>60	113	70	43		
		Gender			
Male	134	133	1	174.955	2.2e-16
Female	366	117	249		
		Pathologic_M			
M0	280	137	143	0	9.90×10^{-01}
M1	9	4	5		
		Pathologic_N			
N0	225	106	119	1.5023,	2.20×10^{-01}
N1	225	120	105		
Pathologic_T					
T1	141	57	84	9.955	1.90×10^{-02}
T2	166	85	81		
T3	168	91	77		
T4	23	16	7		
		Pathologic stage			
I	279	133	146	6.651	8.73×10^{-02}
II	51	24	27		
III	112	56	56		
IV	56	37	19		
		Vital status			
Death	16	9	7	0.061	8.06×10^{-01}
Alive	483	241	242		

Table 2. Correlations between the Hsa-MiR-204−5p Level and Clinical Information

Characteristic total cases	N of case 500	hsa-miR-204−5p level		χ2	P value
		Low (N = 250)	**High** (N = 250)		
		Age (years)			
≤60	387	194	193	0	9.90×10^{-01}
>60	113	56	57		
		Gender			
Male	134	62	72	0.826	3.64×10^{-01}
Female	366	188	178		
		Pathologic_M			
M0	280	148	132	0.025	8.74×10^{-01}
M1	9	4	5		
		Pathologic_N			
N0	225	90	135	22.238	2.41×10^{-06}
N1	225	141	84		
		Pathologic_T			
T1	141	62	79	7.481	5.81×10^{-02}
T2	166	79	87		
T3	168	92	76		
T4	23	16	7		
		Pathologic stage			
I	279	133	146	8.123	4.36×10^{-02}
II	51	21	30		
III	112	58	54		
IV	56	37	19		
		Vital status			
Death	16	7	9	0.061	8.06×10^{-01}
Alive	483	242	241		

stages ($p < 0.05$, Table 1). In addition, the miR-204−5p level was evidently related to pathologic-N stages and pathologic stages ($p < 0.05$, Table 2); also, FN1 expression levels were closely linked to pathologic-N stages, pathologic-T stages, and pathologic stages ($p < 0.05$, Table 3).

https://doi.org/10.1021/acsomega.5c00390
ACS Omega 2025, 10, 19643−19654

Table 3. Correlations between the FN1 Expression and Clinical Information

Characteristic total cases	*N* of case 500	FN1 expression		$\chi 2$	*P* value
		Low (*N* = 250)	**High** (*N* = 250)		
		Age (years)			
≤60	387	197	190	0.412	5.21×10^{-01}
>60	113	53	60		
		Gender			
Male	134	67	67	0	1
Female	366	183	183		
		Pathologic_M			
M0	280	122	158	1.065	3.02×10^{-01}
M1	9	6	3		
		Pathologic_N			
N0	225	142	83	38.769	4.77×10^{-10}
N1	225	75	150		
		Pathologic_T			
T1	141	77	64	25.840	1.03×10^{-05}
T2	166	102	64		
T3	168	65	103		
T4	23	5	18		
		Pathologic stage			
I	279	148	131	26.247	8.47×10^{-06}
II	51	38	13		
III	112	45	67		
IV	56	17	39		
		Vital status			
Death	16	7	9	0.061	8.06×10^{-01}
Alive	483	242	241		

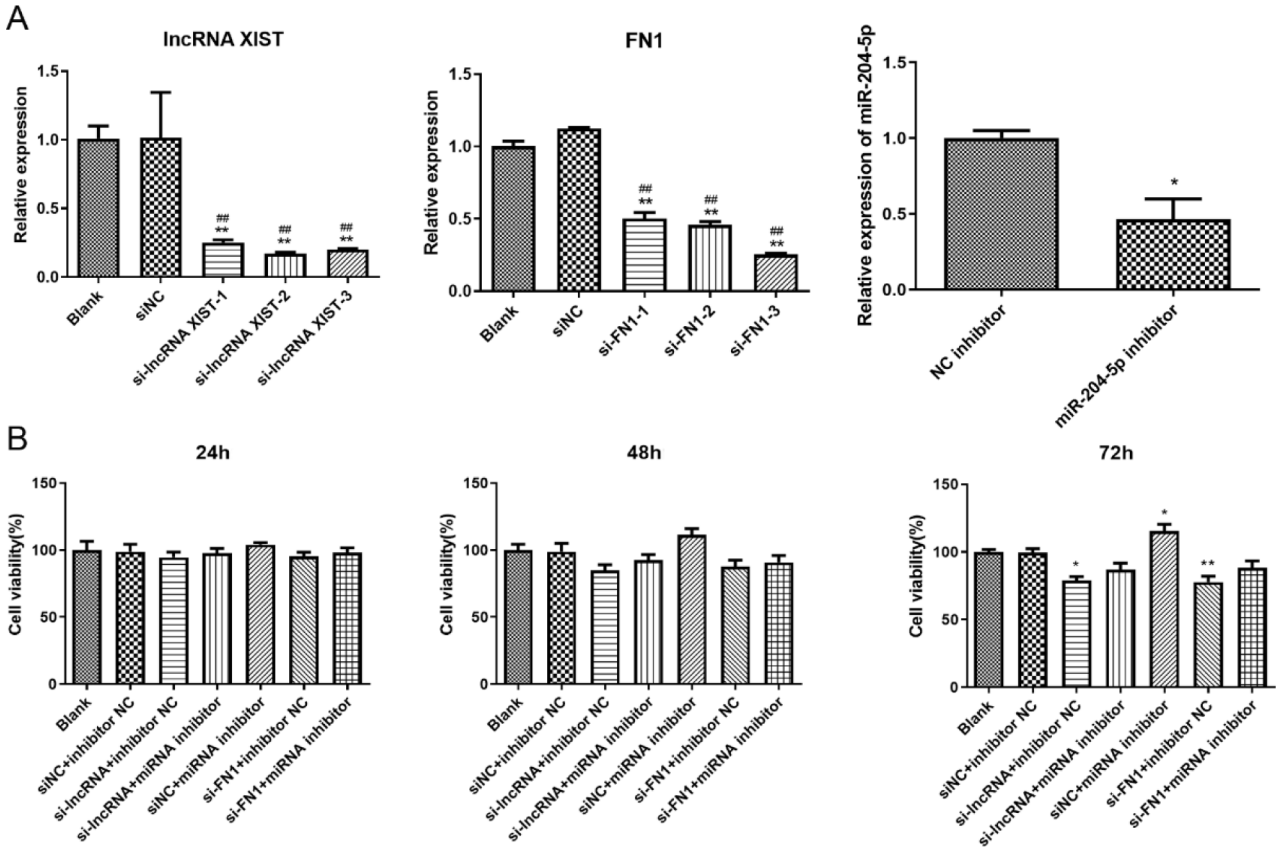

Figure 2. Knockdown of lncRNA XIST or FN1 inhibited PTC cell growth by conducting CCK8 assays. (A) The expression of XIST, FN1, and miR-204−5p was determined by qRT-PCR. (B) The viability of BCPAP cells transfected with si-lncRNA, si-FN1, or miR-204−5p inhibitor using CCK8 assays. * $p < 0.05$, ** $p < 0.01$ compared with blank group or NC inhibitor group; ##, $p < 0.01$ compared with siNC groups.

https://doi.org/10.1021/acsomega.5c00390
ACS Omega 2025, 10, 19643−19654

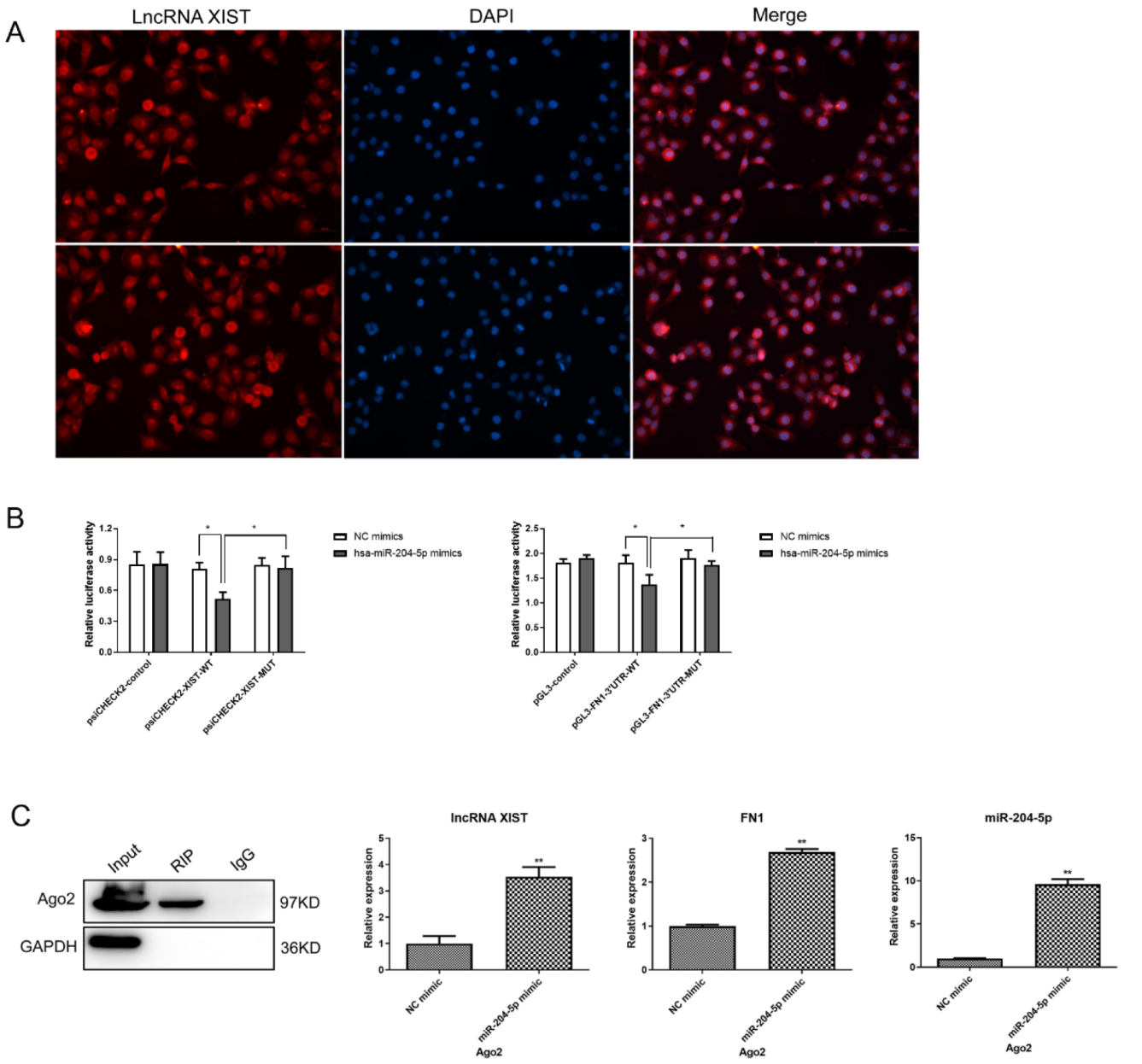

Figure 3. LncRNA XIST functioned in PTC by binding with miR-204−5p. (A) FISH results show lncRNA XIST (in green) cellular distribution in BCPAP cells. (B) Luciferase reporter assay was performed to explore the binding between lncRNA XIST or FN1 with miR-204−5p. (C) RIP assays were performed with an anti-Ago2 antibody after cellular transfection, followed by the expression of qRT-PCR analysis. *$p < 0.05$, ** $p < 0.01$.

LncRNA XIST or FN1 Knockdown Inhibited the Proliferation of Thyroid Cancer Cells. To classify the possible roles of XIST, miR-24−5p, and FN1 in PTC, BCPAP cells were transfected with siRNAs targeting XIST and FN1 or miR-204−5p inhibitor (Figure 2A), and the transfected efficiency was detected. It was found that there were no significant differences in the XIST and FN1 expression between the blank and siNC groups ($p > 0.05$); however, transfection with siRNAs targeting XIST and FN1 significantly downregulated their expression ($p < 0.05$, Figure 2A). Moreover, compared to the NC inhibitor, miR-204−5p inhibitor significantly declined the miR-204−5p level ($p < 0.05$, Figure 2A). According to the qRT-PCR detection results, we selected si-lncRNA XIST-#2 and si-FN1-#3 for the following experiments due to the greatest efficiency to target gene knockdown. CCK8 assay showed that the cell activity was decreased in the lncRNA XIST or FN1 knockdown group after 72 h of treatment, while miR-204−5p inhibitor could partly rescue the cell viability. On the contrary, miR-204−5p suppression displayed increased cell activity, and combing of si-FN1 + miR-204−5p could partly reverse the increase (Figure 2B). Finally, we selected a 72-h treatment time point to carry out the follow study.

LncRNA XIST Serves as a Molecular Sponge of miR-204−5p. We proposed that XIST might could function as a ceRNA to absorb miR-204−5p, thereby affecting FN1 expression in PTC. First, we examined the subcellular location of lncRNA XIST in BCPAP cells since only the lncRNAs in the cytoplasm involves in post-transcriptional regulation.[39] The FISH assay demonstrated that lncRNA XIST was located in the cytoplasm, which could be used as a ceRNA (Figure 3A). The luciferase reporter assay demonstrated that in the cells

https://doi.org/10.1021/acsomega.5c00390
ACS Omega 2025, 10, 19643−19654

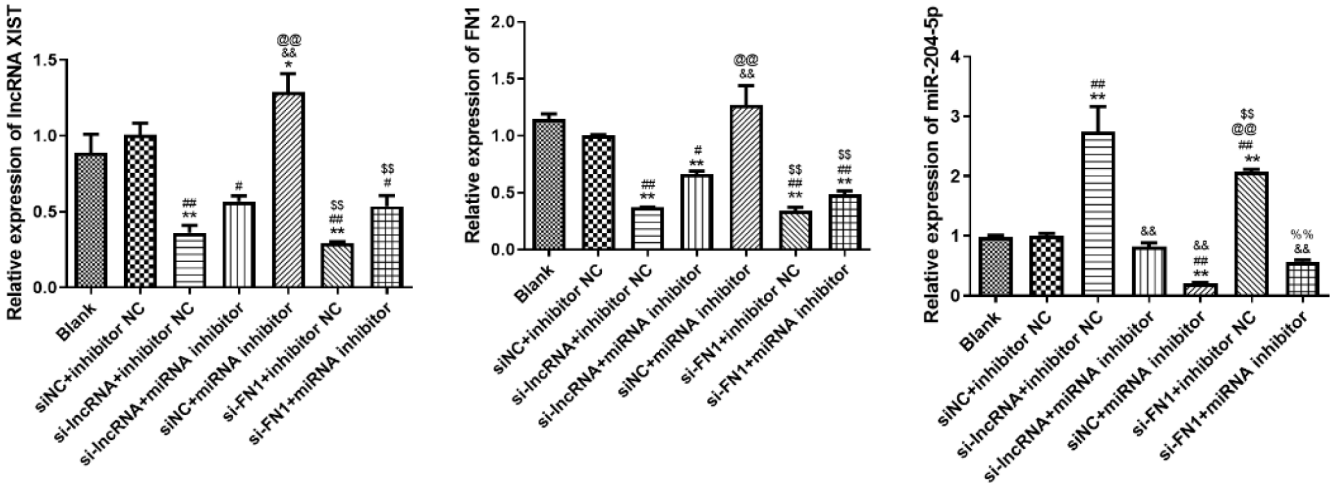

Figure 4. XIST modulated FN1 expression via competitively binding miR-204−5p. *$p < 0.05$, **$p < 0.01$ compared with the blank group; # $p < 0.05$, ## $p < 0.01$ compared with the siNC + inhibitor NC group; and $p < 0.05$, and $p < 0.01$ compared with the si-lncRNA + inhibitor NC group; @@ $p < 0.01$ compared with the si-lncRNA + miRNA inhibitor group; $$ $p < 0.01$ compared with the siNC + miRNA inhibitor group; %%: $p < 0.01$ compared with the si-FN1 + inhibitor NC group.

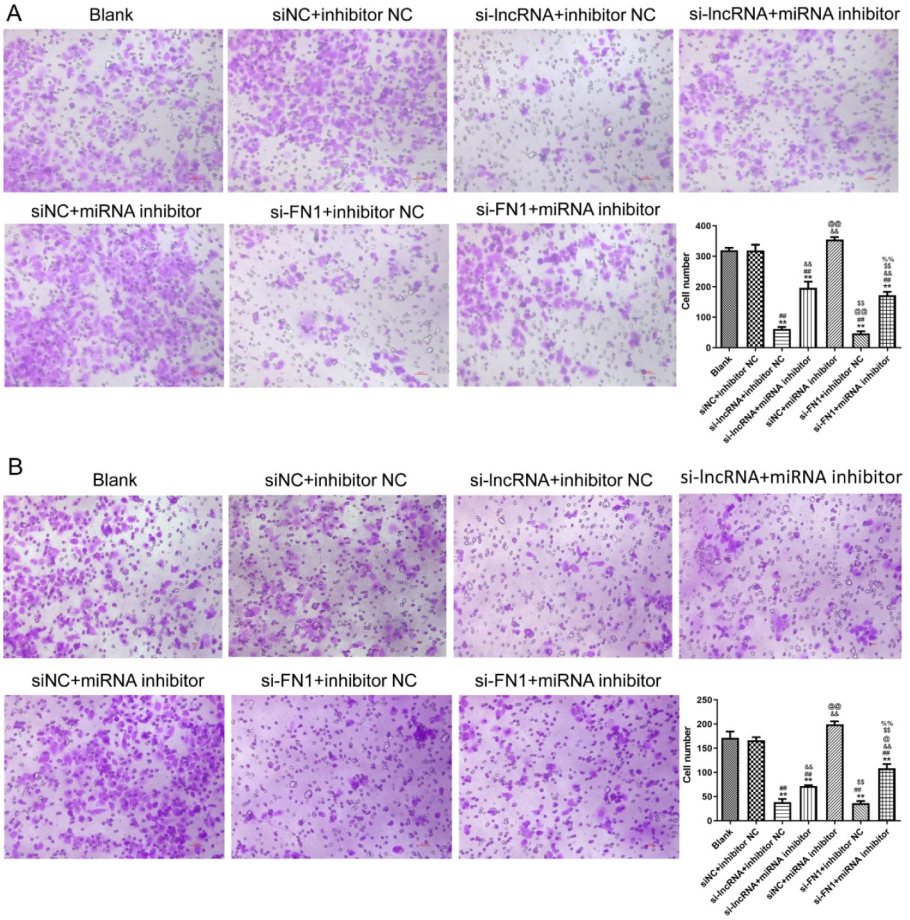

Figure 5. Knockdown of lncRNA XIST or FN1 reduces the metastatic (A) and invasive (B) ability of PTC cells in transwell assay. **$p < 0.01$ compared with the blank group; ## $p < 0.01$ compared with the siNC + inhibitor NC group; and $p < 0.01$ compared with the si-lncRNA + inhibitor NC group; @@ $p < 0.01$ compared with the si-lncRNA + miRNA inhibitor group; $$ $p < 0.01$ compared with the siNC + miRNA inhibitor group; %%: $p < 0.01$ compared with the si-FN1 + inhibitor NC group.

transfected with psiCHECK2-XIST-wide type (WT) or pGL3-FN1-WT plasmids, miR-204−5p mimics significantly suppressed the luciferase activity compared to the NC mimics ($p < 0.05$), but no significant difference in luciferase activity was found in the cells transfected with psiCHECK2-XIST mutant (MUT) or pGL3-FN1-MUT plasmids ($p > 0.05$, Figure 3B). Additionally, RIP assay demonstrated that XIST, FN1, and miR-204−5p displayed enhanced expression levels in the miR-

https://doi.org/10.1021/acsomega.5c00390
ACS Omega 2025, 10, 19643−19654

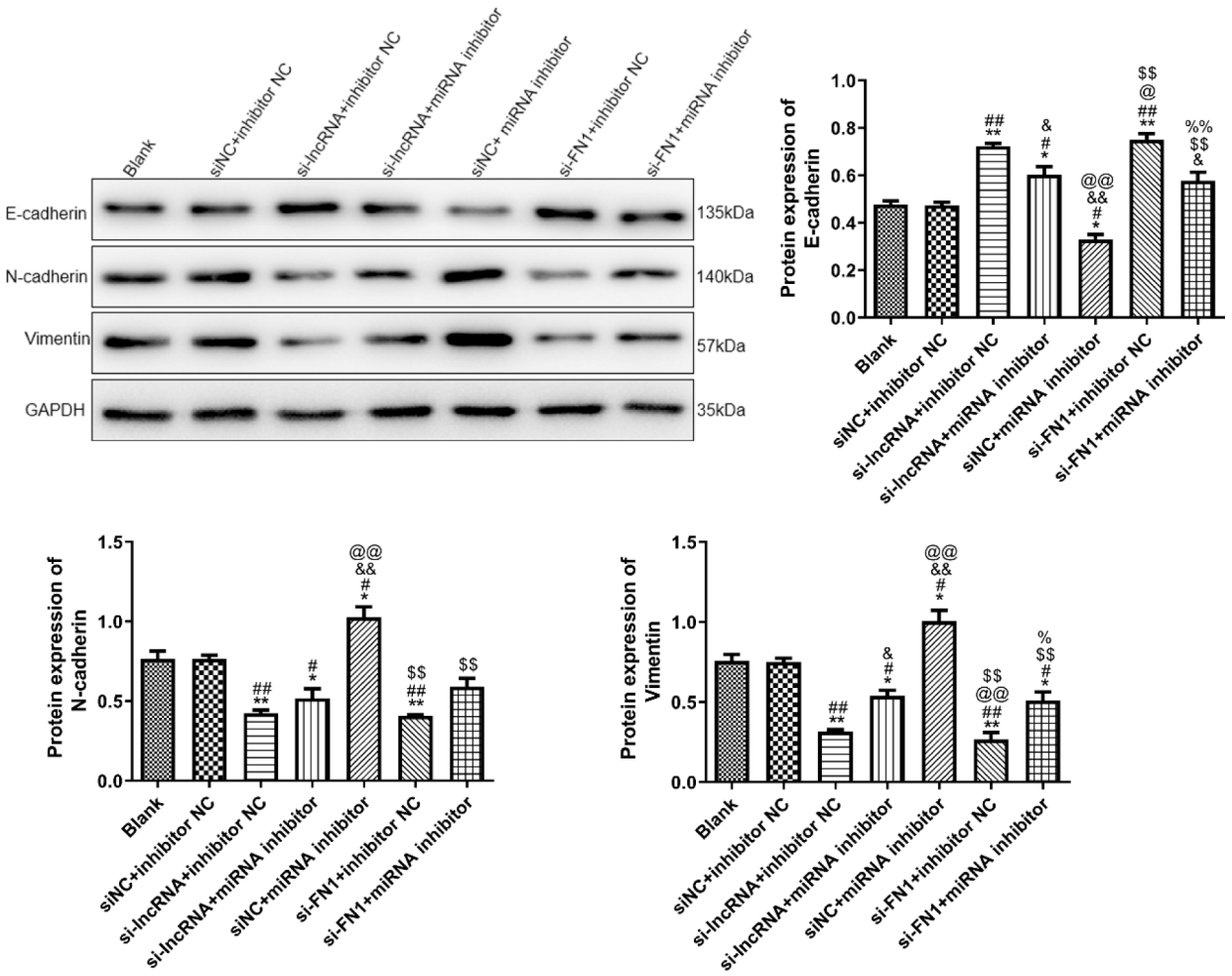

Figure 6. Protein expression of EMT-related proteins (E-cadherin, N-cadherin, and Vimentin) in PTC cells with different transfections using Western blot. * $p < 0.05$, ** $p < 0.01$ compared with the blank group; # $p < 0.05$, ## $p < 0.01$ compared with the siNC + inhibitor NC group; and $p < 0.05$, and $p < 0.01$ compared with the si-lncRNA + inhibitor NC group; @ $p < 0.05$, @@ $p < 0.01$ compared with the si-lncRNA + miRNA inhibitor group; $ $p < 0.05$, $$ $p < 0.01$ compared with the siNC + miRNA inhibitor group; % $p < 0.05$, %%: $p < 0.01$ compared with the si-FN1 + inhibitor NC group.

204−5p mimics of the anti-Ago2 group in comparison with the NC mimics group ($p < 0.01$, Figure 3C). These results indicated the potential interaction among XIST, FN1, and miR-204−5p.

LncRNA XIST Modulated FN1 Expression through Competitively Binding MiR-204−5p in PTC Cells. To determine whether XIST exerts functions through miR-204−5p, we performed rescue experiments by inhibiting miR-204−5p levels using a specific miRNA inhibitor in XIST-knockdown PTC cells. The findings indicated that lncRNA XIST inhibition could considerably decreased the FN1 expression and increase miR-204−5p level in the si-lncRNA group, whereas miR-204−5p inhibitor partially restored the reduction of FN1 level in si-lncRNA+ miRNA inhibitor group cells (Figure 4, $p < 0.01$). Similarly, after inhibition of FN1, the expression of lncRNA XIST was decreased and the expression of miR-204−5p was increased. Whereas, miR-204−5p inhibitor also slightly reversed the reduction of XIST level in si-FN1 + miRNA inhibitor group cells (Figure 4, $p < 0.01$). Finally, the usage of miR-204−5p inhibitor can increase the expressed levels of lncRNA XIST and FN1 in siNC + miRNA inhibitor group cells ($p < 0.01$).

LncRNA XIST/miR-204−5p/FN1 Affected PTC Cell Migration and Invasion. Cell migration assays demonstrated XIST or FN1 knockdown caused the attenuated migration, while inhibition of miR-204−5p boosted cell migration compared to the control groups (Figure 5A, $p < 0.01$). The transwell assay further revealed loss of XIST or FN1 resulted in reduced numbers of cells crossing the upper chamber. In contrast, miR-204−5p inhibitor promotes cell invasion (Figure 5B, $p < 0.01$).

LncRNA XIST/miR-204−5p/FN1 Regulated the Expression of EMT-Related Proteins in PTC Cells. Finally, the effects of lncRNA XIST/miR-204−5p/FN1 on the expression of EMT-related proteins (E-cadherin, N-cadherin, and Vimentin) in PTC cells transfected with siRNAs targeting XIST and FN1 or miR-204−5p inhibitor. No significant differences were observed in the protein expression of E-cadherin, N-cadherin, and Vimentin between the blank and siNC + inhibitor NC groups ($p > 0.05$, Figure 6). Compared with the blank cells, XIST or FN1 knockdown significantly upregulated the E-cadherin expression while downregulated the N-cadherin and Vimentin expression ($p < 0.05$, Figure 6). However, the miR-204−5p inhibitor could evidently partially reverse the actions of XIST or FN1 knockdown in the protein

https://doi.org/10.1021/acsomega.5c00390
ACS Omega 2025, 10, 19643−19654

expression of E-cadherin, N-cadherin, and Vimentin (Figure 6).

DISCUSSION

Due to the continuous increase in the burden of cancer, new treatments are needed. Traditional chemotherapy drugs are often highly toxic, but oncogenes such as BUB1B and c-MYC may be promising alternatives.[40] A previous study has reported that targeting the c-MYC G-quadruplexes can be used in the treatment of small molecule cancers.[41] In addition, over the past few decades, lncRNAs and miRNAs have gained prominence as regulators of cancer and potential prognostic biomarkers. Certain lncRNAs have been identified for their involvement in regulating gene expression across multiple levels, encompassing posttranscriptional processing, RNA maturation, and transport. Multiple studies have specifically investigated the intricate interplay among dysregulated lncRNAs, miRNAs, and mRNAs, constructing cancer-associated ceRNA networks.

XIST serves as a ceRNA to sponge multiple miRNAs, preventing their binding to target mRNAs and thereby influencing the development of various cancer types.[21,22] In this study, we detected a significant upregulation of XIST mRNA in tumor tissues and PTC cell lines. It also have been reported that lncRNA XIST is significantly upregulated in other cancers, such as breast cancer,[42] bladder cancer,[43] and liver cancer.[44] Silencing XIST can suppress PTC progression by inhibiting cell growth, invasion, and metastasis. RIP assays revealed the interaction between XIST and miR-204 in the BCPAP cells. Functional assays also revealed that by sponging miR-204, XIST contributed to the carcinogenicity of PTC, interfering with tumor metastasis and invasion processes. While XIST is canonically considered a tumor suppressor through XCI maintenance,[45] our findings reveal its oncogenic reprogramming in PTC. This functional switch appears driven by (1) thyroid-specific RNA-protein complexes, (2) BRAF mutation-associated posttranslational modifications, and (3) preferential engagement with non-X chromosomal targets. Such plasticity suggests that lncRNA functions cannot be extrapolated across cancer types without empirical validation. In addition, our study, along with others, has observed context-dependent expression patterns of XIST across malignancies,[45,46] presenting both challenges and opportunities for its biomarker application. The potential limitations of using XIST as a biomarker for PTC may be tissue-specific differences, sexual dimorphism, and molecular subtype heterogeneity.

MiR-204, a well-established regulator of numerous target genes, is associated with several cancer progression and clinical stages.[24] It has been previously reported that miR-204−5p is downregulated in PTC and associated with invasiveness. For example, Van Branteghem et al.[27] showed that the inhibition of miR-204−5p on cell invasion in PTC involves the direct binding and inhibition of HMGA2 and EMT. Another study manifested that LINC00704 could promote the proliferation, migration, and invasion of PTC cells through the miR-204−5p/HMGB1 axis.[47] Consistent with these reports, our data also confirmed miR-204−5p downregulation in PTC tissues and demonstrated its suppressive effects on migration and invasion by targeting FN1. Silencing XIST upregulated miR-204−5p expression, suppressed proliferation, autophagy, and enhanced vincristine sensitivity in retinoblastoma cells and glioma.[29,30] The regulatory relationship between XIST and miRNAs was also corroborated by additional studies. For instance, in NSCLC, XIST was identified to support TGF-β-induced EMT, cell invasion, and metastasis through controlling the miR-367/ZEB2 axis.[48] Moreover, XIST knockdown was found to suppress nasopharyngeal carcinoma progression through targeting the miR-148a-3p/ADAM17 axis.[49] In the context of CRC, lncRNA XIST regulated tumor growth, EMT, and chemotherapeutic resistance via different mechanisms, including the miR-125b-2−3p-WEE1 axis and miR-200b-3p/ZEB1 axis.[50,51] Our results also showed that lncRNA XIST knockdown could upregulate E-cadherin expression while downregulating N-cadherin and Vimentin expression, but the miR-204−5p inhibitor could evidently partially reverse these actions. Taken together, we speculate that XIST may be a viable target for PTC therapy, regulating PTC progression through sponging miR-204−5p and influencing the EMT signaling pathway.

FN1 is an ECM glycoprotein involved in cell proliferation, carcinogenesis, and EMT. Our results also proved FN1 as a crucial target of miR-204−5p. Transwell assay confirmed that silencing FN1 inhibited the cell metastasis and invasive ability in PTC, whereas this suppressive effect could be reversed by miRNA inhibitor treatment. Importantly, knockdown of FN1 also inhibits the expression level of XIST and modestly suppresses PTC cell viability, indicating that FN1 is an indispensable mediator in XIST overexpression-mediated PTC progression. Several studies have elucidated the roles and mechanisms of FN1 in thyroid cancer. Overexpression of FN1 has been consistently observed in metastasized PTC, particularly in samples harboring BRAF (V600E) mutations, and its upregulation has been positively associated with metastatic lymph node.[52] In vitro assays have demonstrated that elevated FN1 levels promote PTC cell proliferation, migration, and invasion, making FN1 a valuable diagnostic biomarker for predicting PTC lymph node metastasis.[53] Moreover, FN1 has been implicated as a critical factor in PTC cells resistant to BRAF blockade. Following BRAFi treatment in thyroid cancer, both extracellular matrix FN1 and secreted FN1 levels increased, promoting an invasive phenotype via EGR1 activation.[54] Notably, coinhibition of ERK1/2 and BRAF substantially reduced circulating FN1 levels, demonstrating tumor inhibitory effects in a BRAFi-resistant xenograft model.[54] FN1 serves as a direct target of several miRNAs, with its transcript being influenced by various other miRNAs and upstream molecules in cancer progression. For instance, miR-204 has been shown to directly inhibit FN1 mRNA and protein expression, consequently suppressing tumor growth and invasion in renal cell carcinoma,[55] osteosarcoma,[56] and hepatocellular carcinoma.[57] Additionally, miR-142−3p has been found to interact with FN1, suppressing the progression of PTC by inactivating ERK/PI3K signaling.[58] Furthermore, BAG5 upregulates FN1 translational levels by suppressing miR-144−3p, thereby promoting the invasion of PTC cells.[59] Similarly, TRIM29 modulates the FN1 mRNA stability by regulating miR-873−5p level in PTC cells, thereby contributing to cell migration and invasion.[60]

However, the current stage of our study has several limitations. First, the potential upstream regulators of XIST, other alternative regulatory pathways that might influence XIST's roles, and what factors might contribute to its overexpression in PTC should be assessed in the future. Second, further experiments, such as a CRISPR/Cas9-mediated knockout of XIST or FN1 in PTC cells, should be conducted to investigate the specificity of XIST and FN1;

https://doi.org/10.1021/acsomega.5c00390
ACS Omega 2025, 10, 19643−19654

complementary gain-of-function assays should be performed to further validate the oncogenic role of XIST in PTC. Third, further experiments should be carried out to unearth the FDA-approved FN1 pathway inhibitors (such as defactinib) in PTC models. Fourth, whether there are feedback loops regulate the expression of XIST and FN1 needs to be further studied; moreover, the epigenetic modifications of XIST in PTC samples should be assessed. Fifth, other potential miRNA targets that might contribute to FN1 regulation and other ECM-related proteins should be investigated. Moreover, whether silencing XIST enhances sensitivity to BRAF inhibitors in PTC cells, as well as whether the XIST/miR-204−5p/FN1 axis is influenced by external factors such as hypoxia, inflammation, or other tumor microenvironmental conditions, also needs to be considered in the future. While our study cannot fully exclude off-target effects, our data support the targeted efficacy of XIST/FN1 silencing in PTC. Future work will include transcriptome-wide profiling (such as RNA-seq) to comprehensively assess off-target impacts and additional cell lines and in vivo models to evaluate long-term consequences. Given the clinical need for noninvasive PTC diagnostics, further investigation of XIST, miR-204−5p, and FN1 as circulating biomarkers is warranted. Additionally, our conclusions need to be verified in the future to differentiate the oncogenic role of XIST in PTC from its reported tumor-suppressive functions in other cancer types.

In conclusion, our results demonstrated that XIST could serve as an oncogene in PTC, facilitate disease progression via acting as a ceRNA to sponge miR-204−5p, and attenuate the suppressive effect on FN1. The XIST/miR-204−5p/FN1 axis could modulate tumor growth, metastasis, and invasion. Our findings uncovered a possible therapeutic target and diagnostic biomarker for PTC, providing novel insights into the function of lncRNA-XIST in PTC progression.

MATERIALS AND METHODS

Data Download and Bioinformatics Analysis. The expression data of thyroid cancer were downloaded from the TCGA database, and the tumor samples with the histological type of PTC were retained. A total of 500 related samples were obtained. Then, the expression levels of XIST, hsa-miR-204−5p, and FN1 were extracted from the expression levels, and associated clinical information was obtained. Subsequently, all the samples were respectively divided into low-level and high-level expression groups based on the median expression levels of XIST, hsa-miR-204−5p, and FN1.[61] The chi-square test was used to statistically analyze the distribution differences of each clinical factor in different expression level groups.[62]

Clinical PTC Tissue Samples. PTC patients' matched tumor tissue samples (n = 20) and normal adjacent samples (n = 20) were taken after surgical excision at the Affiliated Hospital of Qingdao University. Written informed consent was obtained from all included patients prior to the commencement of the study, and this study was approved by the Ethics Committee of Affiliated Hospital of Qingdao University (Qingdao, Shandong, China). Tissue samples were immediately frozen and kept in liquid nitrogen. Pathological detection was carried out for PTC confirmation. The mRNA expressed level of XIST, FN1, and miR-204−5p in all PTC tissues was determined via qRT-PCR assay.

Cell Resources and Reagents. Thyroid cancer cell lines (BCPAP, TPC-1, and KTC-1) were derived from the Chinese Academy of Sciences Stem Cell Bank. The whole cell lines were cultured in RPMI 1640 (Invitrogen, USA), with 10% fetal bovine serum (FBS; Invitrogen, USA) and a 1% penicillin/streptomycin mixture (Gibco, USA) added as supplements. All cell lines were kept at 37 °C in 5% CO_2 conditions.

CCK-8 Assay. BCPAP cells were seeded in 96-well plates at a density of 1×10^4 cells per well for 24 h, and then, the cells were transfected using si-lncRNA and NC mimics according to the Lipofectamine 3000 kit instructions. Moreover, 10 μL of CCK-8 solution was added to each well and incubated at 37 °C for 1−4 h (OD $\leq$ 2.0). The absorbance per well was measured at 450 nm to assess cell viability.

Cell Transfection. MiR-204−5p mimics and inhibitors, small interfering RNAs (siRNAs) targeted to XIST or FN1 (si-lncRNA and si-FN1), and control siRNA (si-NC) were purchased from Generay Biotechnology (Shanghai, China). For cellular transfections, lipofectamine 3000 (Invitrogen, CA, USA) was used as directed by the manufacturer instruction. Interference efficiency of lncRNA XIST and FN1 was determined by using RT-qPCR.

Quantitative Real-Time PCR. As instructions directed, Takara RNAiso Plus (TaKaRa Bio, Dalian, China) was used to extract total RNAs from PTC cells. Using a PrimeScript II cDNA Synthesis Kit (TaKaRa Bio, Dalian, China), the isolated RNA was synthesized to form the first strand of cDNA. A PrimeScript RT Master Mix (TaKaRa Bio, Dalian, China) was used for reverse transcription. Two phases of the miRNA real-time quantitation experiment were real-time PCR and stem-loop RT.

The primers were synthesized at Shanghai Sangon Biotech Inc. The list of primer sequences include the following: universal stem-loop downstream primer: GTGCAGGGTCC-GAGGT; hsa-U6-RT: GTCGTATCCAGTGCAGGGTCC-GAGGTATTCGCAC TGGATACGACAAAATATG; hsa-U6 forward, CTCGCTTCGGCAGCACA, and reverse, AACGCTTCACGAATTTGCGT; GAPDH forward, TGA-CAACTTTGGTATCGTGGAAGG, and reverse, AGG-CAGGGATGATGTTCTGG AGAG; XIST forward, GACA-CAAGGCCAACGACCTA, and reverse, TCGCTTGGGTCC TCTATCCA; hsa-miR-204−5p forward: GCGCGTTCCCTTTGTCATCCT, and reverse, GTCGTATCCAGTGCAGGGTCCGAGGTATTCG-CACTGGATACGACAGGCAT. The expression levels of miRNA and mRNA were normalized to U6-small nuclear RNA and GAPDH using the $2^{-\Delta\Delta Ct}$ method.

Fluorescence In Situ Hybridization. Fluorescein amidite-labeled lncRNA XIST probes were designed and synthesized by RiboBio (Guangzhou, China). A FISH Kit (RiboBio) was used to detect probe signals according to the manufacturer's instructions. Nuclei were stained with DAPI. All images were acquired on a confocal microscope system (Olympus, Japan).

Luciferase Reporter Assay. A luciferase reporter assay was performed in 293T cells, as described elsewhere. Briefly, the wild-type (WT) and mutant (Mut) binding sites of the 3′-untranslated regions (UTR) of lncRNA XIST and FN1 for hsa-miR-204−5p were amplified using PCR and were introduced into the psiCHECK2 and Pgl3 luciferase expression vectors, respectively (Promega Corporation). 293T cells were cotransfected with 0.4 μg of psiCHECK2-control, psi-CHECK2-XIST-WT, psiCHECK2-XIST-MUT, pGL3-control, pGL3-FN1-WT or pGL3-FN1-MUT and 100 nM hsa-miR-204−5p mimics or NC mimics (Shanghai Tuoran Biotechnology Co., LTD, China) using Lipofectamine 3000 (Thermo

https://doi.org/10.1021/acsomega.5c00390
ACS Omega 2025, 10, 19643−19654

Fisher Scientific, USA) at 37 °C. At 48 h post transfection, luciferase activities were measured using the dual-luciferase reporter assay system (Promega Corporation) according to the manufacturer's protocol. Firefly luciferase activities were normalized to Renilla luciferase activities.

RNA Immunoprecipitation Assay. RIP assays were carried out using the Magna RIP immunoprecipitation kit (Millipore, USA) based on manufacturer's instructions. Collected PTC cells were lysed and incubated with anti-Ago2 (Abcam, MA, USA) or negative rabbit IgG antibody (Abcam, MA, USA) at 4 °C overnight. The cell lysates were kept with magnetic beads conjugated to the corresponding antibodies. The coprecipitated RNA was isolated and further quantified using qRT-PCR.

Cell Migration and Invasion Assays. Transwell chamber system (Jet Biofil, Corp., Guangzhou, China) was utilized for cell migration detection. The si-XIST and si-FN1 PTC cells were reconstituted in 3 mL of FBS-free medium and seeded in the upper chamber at a density of 5×10^5 cells/well. The lower chambers were filled with 10% FBS-containing 500 μL of complement medium. After 48 h of incubation, the whole cells were fixed with 4% formaldehyde and colored with crystal violet dye. Using a cotton swab, the unpenetrated cells on the upper chamber surface were carefully removed off the membrane. The imaged cells were captured using an optical microscope.

For the cell invasion assays, the top Transwell chambers were precoated with Matrigel (BD Biosciences, USA), and the following procedure was similar to the above description in the migration assay.

Western Blot. Total protein was isolated from the cells using RIPA lysis buffer and then quantified using a BCA protein assay kit (Beyotime, Shanghai, China). Then, the protein samples (20 μg) were separated by SDS-PAGE, and the mixture was transferred to PVDF membranes. After blocking with 5% skim milk at 37 °C for 2 h, the membranes were incubated with anti-E-cadherin antibody (1:1000, Proteintech, Wuhan, China), anti-N-cadherin antibody (1:500, Boster, Wuhan, China), anti-Vimentin antibody (1:1000, Proteintech), and anti-GAPDH antibody (1:5000, Proteintech) overnight at 4 °C. After that, the membranes were incubated with the horseradish peroxidase (HPR)-labeled secondary antibodies (goat antimouse/rabbit IgG/HRP, 1:5000, Jackson ImmunoResearch, USA) for 1 h at room temperature. Finally, the protein bands were developed by using a Millipore electrochemical luminescence (ECL) assay kit (Thermo Fisher Scientific, USA).

Statistical Analysis. Data of this study were generated by GraphPad Prism 8.0 (Graphpad Software, CA, USA). Each experiment was carried out for three times, and the results are shown as mean values ± standard deviations. The Student's t test was utilized to assess the differences between two groups. One-way analysis of variance was performed to compare differences among more than two groups. Differences were considered statistically significant with a P value of less than 0.05.

AUTHOR INFORMATION

Corresponding Author

Wenwei Zhang − *Department of Radiology, The Affiliated Hospital of Qingdao University, Qingdao 266003, China;* orcid.org/0009-0005-1236-9475; Phone: +86-0532-82913093; Email: zhangww98@126.com

Authors

Jie Qiu − *Department of Otolaryngology, The Affiliated Hospital of Qingdao University, Qingdao 266003, China*

Maolin Sun − *Department of Otolaryngology, Huangdao District Traditional Chinese Medicine Hospital, Qingdao City, Qingdao 266003, China*

Zuorong Qin − *Department of Otolaryngology, The Affiliated Hospital of Qingdao University, Qingdao 266003, China*

Mingbo Liu − *Department of Otolaryngology, Hainan Hospital of PLA General Hospital, Sanya 572000, China*

Complete contact information is available at: https://pubs.acs.org/10.1021/acsomega.5c00390

Notes

The authors declare no competing financial interest.

ACKNOWLEDGMENTS

This work was supported by the Hainan Provincial Department of Science and Technology under Grant No. HN01ENT07.

ABBREVIATIONS:

ATCC	American Type Culture Collection
ceRNA	competing endogenous RNA
ECM	extracellular matrix
EMT	epithelial-mesenchymal transition;
FN1	fibronectin 1
lncRNA	long noncoding RNA;
PTC	papillary thyroid carcinoma

REFERENCES

(1) Toraih, E. A.; Hussein, M. H.; Zerfaoui, M.; Attia, A. S.; Marzouk Ellythy, A.; Mostafa, A.; Ruiz, E. M. L.; Shama, M. A.; Russell, J. O.; Randolph, G. W. Site-Specific Metastasis and Survival in Papillary Thyroid Cancer: The Importance of Brain and Multi-Organ Disease. *Cancers* **2021**, *13* (7), 1625.

(2) Pacini, F.; Ito, Y.; Luster, M.; Pitoia, F.; Robinson, B.; Wirth, L. Radioactive iodine-refractory differentiated thyroid cancer: unmet needs and future directions. *Expert Rev. Endocrinol. Metab.* **2012**, *7* (5), 541−554.

(3) Lin, Y.; Qin, S.; Li, Z.; Yang, H.; Fu, W.; Li, S.; Chen, W.; Gao, Z.; Miao, W.; Xu, H. Apatinib vs Placebo in Patients With Locally Advanced or Metastatic, Radioactive Iodine-Refractory Differentiated Thyroid Cancer: The REALITY Randomized Clinical Trial. *JAMA Oncology* **2022**, *8* (2), 242−250.

(4) Plath, K.; Mlynarczyk-Evans, S.; Nusinow, D. A.; Panning, B. Xist RNA and the mechanism of X chromosome inactivation. *Annu. Rev. Genet.* **2002**, *36*, 233−278.

(5) Engreitz, J. M.; Pandya-Jones, A.; McDonel, P.; Shishkin, A.; Sirokman, K.; Surka, C.; Kadri, S.; Xing, J.; Goren, A.; Lander, E. S. The Xist lncRNA exploits three-dimensional genome architecture to spread across the X chromosome. *Science* **2013**, *341* (6147), 1237973.

(6) McHugh, C. A.; Chen, C. K.; Chow, A.; Surka, C. F.; Tran, C.; McDonel, P.; Pandya-Jones, A.; Blanco, M.; Burghard, C.; Moradian, A. The Xist lncRNA interacts directly with SHARP to silence transcription through HDAC3. *Nature* **2015**, *521* (7551), 232−236.

(7) Sun, Z.; Zhang, B.; Cui, T. Long non-coding RNA XIST exerts oncogenic functions in pancreatic cancer via miR-34a-5p. *Oncol. Rep.* **2018**, *39* (4), 1591−1600.

(8) Wu, X.; Dinglin, X.; Wang, X.; Luo, W.; Shen, Q.; Li, Y.; Gu, L.; Zhou, Q.; Zhu, H.; Li, Y. Long noncoding RNA XIST promotes malignancies of esophageal squamous cell carcinoma via regulation of miR-101/EZH2. *Oncotarget* **2017**, *8* (44), 76015−76028.

(9) Yang, X.; Zhang, S.; He, C.; Xue, P.; Zhang, L.; He, Z.; Zang, L.; Feng, B.; Sun, J.; Zheng, M. METTL14 suppresses proliferation and

metastasis of colorectal cancer by down-regulating oncogenic long non-coding RNA XIST. *Mol. Cancer* **2020**, *19* (1), 46.
(10) Xiao, D.; Cui, X.; Wang, X. Long noncoding RNA XIST increases the aggressiveness of laryngeal squamous cell carcinoma by regulating miR-124−3p/EZH2. *Exp. Cell Res.* **2019**, *381* (2), 172−178.
(11) Sun, Y.; Xu, J. TCF-4 Regulated lncRNA-XIST Promotes M2 Polarization Of Macrophages And Is Associated With Lung Cancer. *OncoTargets Ther.* **2019**, *12*, 8055−8062.
(12) Wang, H.; Shen, Q.; Zhang, X.; Yang, C.; Cui, S.; Sun, Y.; Wang, L.; Fan, X.; Xu, S. The Long Non-Coding RNA XIST Controls Non-Small Cell Lung Cancer Proliferation and Invasion by Modulating miR-186−5p. *Cell. Physiol. Biochem.* **2017**, *41* (6), 2221−2229.
(13) Cheng, Z.; Li, Z.; Ma, K.; Li, X.; Tian, N.; Duan, J.; Xiao, X.; Wang, Y. Long Non-coding RNA XIST Promotes Glioma Tumorigenicity and Angiogenesis by Acting as a Molecular Sponge of miR-429. *J. Cancer* **2017**, *8* (19), 4106−4116.
(14) Yu, H.; Xue, Y.; Wang, P.; Liu, X.; Ma, J.; Zheng, J.; Li, Z.; Li, Z.; Cai, H.; Liu, Y. Knockdown of long non-coding RNA XIST increases blood-tumor barrier permeability and inhibits glioma angiogenesis by targeting miR-137. *Oncogenesis* **2017**, *6* (3), No. e303.
(15) Cheng, Z.; Luo, C.; Guo, Z. LncRNA-XIST/microRNA-126 sponge mediates cell proliferation and glucose metabolism through the IRS1/PI3K/Akt pathway in glioma. *J. Cell. Biochem.* **2020**, *121* (3), 2170−2183.
(16) Ma, Y.; Zhu, Y.; Shang, L.; Qiu, Y.; Shen, N.; Wang, J.; Adam, T.; Wei, W.; Song, Q.; Li, J. LncRNA XIST regulates breast cancer stem cells by activating proinflammatory IL-6/STAT3 signaling. *Oncogene* **2023**, *42* (18), 1419−1437.
(17) Zhao, Y.; Yu, Z.; Ma, R.; Zhang, Y.; Zhao, L.; Yan, Y.; Lv, X.; Zhang, L.; Su, P.; Bi, J. lncRNA-Xist/miR-101−3p/KLF6/C/EBPα axis promotes TAM polarization to regulate cancer cell proliferation and migration. *Molecular Therapy. Nucleic Acids* **2021**, *23*, 536−551.
(18) Yildirim, E.; Kirby, J. E.; Brown, D. E.; Mercier, F. E.; Sadreyev, R. I.; Scadden, D. T.; Lee, J. T. Xist RNA is a potent suppressor of hematologic cancer in mice. *Cell* **2013**, *152* (4), 727−742.
(19) Sun, K.; Jia, Z.; Duan, R.; Yan, Z.; Jin, Z.; Yan, L.; Li, Q.; Yang, J. Long non-coding RNA XIST regulates miR-106b-5p/P21 axis to suppress tumor progression in renal cell carcinoma. *Biochem. Biophys. Res. Commun.* **2019**, *510* (3), 416−420.
(20) Guo, T.; Yuan, D.; Zhang, W.; Zhu, D.; Xiao, A.; Mao, G.; Jiang, W.; Lin, M.; Wang, J. Upregulation of long noncoding RNA XIST has anticancer effects on ovarian cancer through sponging miR-106a. *Human Cell.* **2021**, *34* (2), 579−587.
(21) Xu, Y.; Wang, J.; Wang, J. Long noncoding RNA XIST promotes proliferation and invasion by targeting miR-141 in papillary thyroid carcinoma. *Onco Targets Ther.* **2018**, *11*, 5035−5043.
(22) Du, Y. L.; Liang, Y.; Cao, Y.; Liu, L.; Li, J.; Shi, G. Q. LncRNA XIST Promotes Migration and Invasion of Papillary Thyroid Cancer Cell by Modulating MiR-101−3p/CLDN1 Axis. *Biochem. Genet.* **2021**, *59* (2), 437−452.
(23) Cai, T.; He, Y.; Peng, B. lncRNA XIST Stimulates Papillary Thyroid Cancer Development through the miR-330−3p/PDE5A Axis. *Crit Rev. Eukaryot Gene Expr.* **2023**, *33* (3), 13−26.
(24) Liu, L.; Wang, J.; Li, X.; Ma, J.; Shi, C.; Zhu, H.; Xi, Q.; Zhang, J.; Zhao, X.; Gu, M. MiR-204−5p suppresses cell proliferation by inhibiting IGFBP5 in papillary thyroid carcinoma. *Biochem. Biophys. Res. Commun.* **2015**, *457* (4), 621−626.
(25) Hong, B. S.; Ryu, H. S.; Kim, N.; Kim, J.; Lee, E.; Moon, H.; Kim, K. H.; Jin, M. S.; Kwon, N. H.; Kim, S. Tumor Suppressor miRNA-204−5p Regulates Growth, Metastasis, and Immune Microenvironment Remodeling in Breast Cancer. *Cancer Res.* **2019**, *79* (7), 1520−1534.
(26) Gu, Y.; Zhang, X.; Li, Y.; Shi, J.; Cui, H.; Ren, Y.; Liu, S.; Qiao, Y.; Cheng, Y.; Liu, Y. MiR-204−5p-targeted AP1S2 is necessary for papillary thyroid carcinoma. *Mol. Cell. Endocrinol.* **2023**, *574*, 111993.
(27) Van Branteghem, C.; Augenlicht, A.; Demetter, P.; Craciun, L.; Maenhaut, C. Unraveling the Roles of miR-204−5p and HMGA2 in Papillary Thyroid Cancer Tumorigenesis. *Int. J. Mol. Sci.* **2023**, *24* (13), 10764.
(28) Stojanović, S.; Dobrijević, Z.; Šelemetjev, S.; Đorić, I.; Janković Miljuš, J.; Živaljević, V.; Išić Denčić, T. MiR-203a-3p, miR-204−3p, miR-222−3p as useful diagnostic and prognostic tool for thyroid neoplasia spectrum. *Endocrine* **2023**, *79* (1), 98−112.
(29) Shen, J.; Xiong, J.; Shao, X.; Cheng, H.; Fang, X.; Sun, Y.; Di, G.; Mao, J.; Jiang, X. Knockdown of the long noncoding RNA XIST suppresses glioma progression by upregulating miR-204−5p. *J. Cancer* **2020**, *11* (15), 4550−4559.
(30) Yao, L.; Yang, L.; Song, H.; Liu, T. G.; Yan, H. Silencing of lncRNA XIST suppresses proliferation and autophagy and enhances vincristine sensitivity in retinoblastoma cells by sponging miR-204−5p. *Eur. Rev. Med. Pharmacol. Sci.* **2020**, *24* (7), 3526−3537.
(31) Lu, G.; Tian, P.; Zhu, Y.; Zuo, X.; Li, X. LncRNA XIST knockdown ameliorates oxidative low-density lipoprotein-induced endothelial cells injury by targeting miR-204−5p/TLR4. *J. Biosci.* **2020**, *45*, 52.
(32) Qiu, J.; Zhang, W.; Zang, C.; Liu, X.; Liu, F.; Ge, R.; Sun, Y.; Xia, Q. Identification of key genes and miRNAs markers of papillary thyroid cancer. *Biol. Res.* **2018**, *51* (1), 45.
(33) Lenselink, E. A. Role of fibronectin in normal wound healing. *Int. Wound J.* **2015**, *12* (3), 313−316.
(34) Griggs, L. A.; Hassan, N. T.; Malik, R. S.; Griffin, B. P.; Martinez, B. A.; Elmore, L. W.; Lemmon, C. A. Fibronectin fibrils regulate TGF-β1-induced Epithelial-Mesenchymal Transition. *Matrix Biol.* **2017**, *60−61*, 157−175.
(35) Dalton, C. J.; Lemmon, C. A. Fibronectin: Molecular Structure, Fibrillar Structure and Mechanochemical Signaling. *Cells* **2021**, *10* (9), 2443.
(36) Potts, J. R.; Campbell, I. D. Structure and function of fibronectin modules. *Matrix Biol.* **1996**, *15* (5), 313−320.
(37) Lin, T. C.; Yang, C. H.; Cheng, L. H.; Chang, W. T.; Lin, Y. R.; Cheng, H. C. Fibronectin in Cancer: Friend or Foe. *Cells* **2020**, *9* (1), 27.
(38) Farooq, F.; Amin, A.; Wani, U. M.; Lone, A.; Qadri, R. A. Shielding and nurturing: Fibronectin as a modulator of cancer drug resistance. *J. Cell. Physiol.* **2023**, *238* (8), 1651−1669.
(39) Gao, N.; Li, Y.; Li, J.; Gao, Z.; Yang, Z.; Li, Y.; Liu, H.; Fan, T. Long Non-Coding RNAs: The Regulatory Mechanisms, Research Strategies, and Future Directions in Cancers. *Front. Oncol.* **2020**, *10*, 598817.
(40) Mishra, D.; Mishra, A.; Rai, S. N.; Singh, S. K.; Vamanu, E.; Singh, M. P. In Silico Insight to Identify Potential Inhibitors of BUB1B from Mushroom Bioactive Compounds to Prevent Breast Cancer Metastasis. *Front. Biosci.* **2023**, *28* (7), 151.
(41) Thumpati, P.; Rai, S. N.; Prajapati, C.; Ramakrishna, K.; Singh, S. K. Targeting C-MYC G-Quadruplexes For Cancer Treatment With Small Molecules. *Sci. Pharm.* **2025**, *93* (1), 6.
(42) Zong, Y.; Zhang, Y.; Hou, D.; Xu, J.; Cui, F.; Qin, Y.; Sun, X. The lncRNA XIST promotes the progression of breast cancer by sponging miR-125b-5p to modulate NLRC5. *Am. J. Transl. Res.* **2020**, *12* (7), 3501−3511.
(43) Kong, Y. L.; Wang, H. D.; Gao, M.; Rong, S. Z.; Li, X. X. LncRNA XIST promotes bladder cancer progression by modulating miR-129−5p/TNFSF10 axis. *Discover Oncology* **2024**, *15* (1), 65.
(44) Liu, L.; Jiang, H.; Pan, H.; Zhu, X. LncRNA XIST promotes liver cancer progression by acting as a molecular sponge of miR-200b-3p to regulate ZEB1/2 expression. *J. Int. Med. Res.* **2021**, *49* (5), 3000605211016211.
(45) Richart, L.; Picod-Chedotel, M. L.; Wassef, M.; Macario, M.; Aflaki, S.; Salvador, M. A.; Héry, T.; Dauphin, A.; Wicinski, J.; Chevrier, V.; et al. XIST loss impairs mammary stem cell differentiation and increases tumorigenicity through Mediator hyperactivation. *Cell* **2022**, *185* (12), 2164−2183.e25.
(46) Wang, K.; Bhattacharya, A.; Haratake, N.; Daimon, T.; Nakashoji, A.; Ozawa, H.; Peng, B.; Li, W.; Kufe, D. XIST and MUC1-C form an auto-regulatory pathway in driving cancer progression. *Cell Death Dis.* **2024**, *15* (5), 330.

https://doi.org/10.1021/acsomega.5c00390
ACS Omega 2025, 10, 19643−19654

(47) Lin, Y.; Jiang, J. Long non-coding RNA LINC00704 promotes cell proliferation, migration, and invasion in papillary thyroid carcinoma via miR-204−5p/HMGB1 axis. *Open Life Sci.* **2020**, *15* (1), 561−571.
(48) Li, C.; Wan, L.; Liu, Z.; Xu, G.; Wang, S.; Su, Z.; Zhang, Y.; Zhang, C.; Liu, X.; Lei, Z. Long non-coding RNA XIST promotes TGF-β-induced epithelial-mesenchymal transition by regulating miR-367/141-ZEB2 axis in non-small-cell lung cancer. *Cancer Lett.* **2018**, *418*, 185−195.
(49) Shi, J.; Tan, S.; Song, L.; Song, L.; Wang, Y. LncRNA XIST knockdown suppresses the malignancy of human nasopharyngeal carcinoma through XIST/miRNA-148a-3p/ADAM17 pathway in vitro and in vivo. *Biomed. Pharmacother.* **2020**, *121*, 109620.
(50) Zeng, Z. L.; Lu, J. H.; Wang, Y.; Sheng, H.; Wang, Y. N.; Chen, Z. H.; Wu, Q. N.; Zheng, J. B.; Chen, Y. X.; Yang, D. D. The lncRNA XIST/miR-125b-2−3p axis modulates cell proliferation and chemotherapeutic sensitivity via targeting Wee1 in colorectal cancer. *Cancer Med.* **2021**, *10* (7), 2423−2441.
(51) Chen, D. L.; Chen, L. Z.; Lu, Y. X.; Zhang, D. S.; Zeng, Z. L.; Pan, Z. Z.; Huang, P.; Wang, F. H.; Li, Y. H.; Ju, H. Q. Long noncoding RNA XIST expedites metastasis and modulates epithelial-mesenchymal transition in colorectal cancer. *Cell Death Dis.* **2017**, *8* (8), No. e3011.
(52) Xia, S.; Wang, C.; Postma, E. L.; Yang, Y.; Ni, X.; Zhan, W. Fibronectin 1 promotes migration and invasion of papillary thyroid cancer and predicts papillary thyroid cancer lymph node metastasis. *OncoTargets Ther.* **2017**, *10*, 1743−1755.
(53) Sponziello, M.; Rosignolo, F.; Celano, M.; Maggisano, V.; Pecce, V.; De Rose, R. F.; Lombardo, G. E.; Durante, C.; Filetti, S.; Damante, G. Fibronectin-1 expression is increased in aggressive thyroid cancer and favors the migration and invasion of cancer cells. *Mol. Cell. Endocrinol.* **2016**, *431*, 123−132.
(54) Hicks, H. M.; Pozdeyev, N.; Sams, S. B.; Pugazhenthi, U.; Bales, E. S.; Hofmann, M. C.; McKenna, L. R.; Schweppe, R. E. Fibronectin Contributes to a BRAF Inhibitor-driven Invasive Phenotype in Thyroid Cancer through EGR1, Which Can Be Blocked by Inhibition of ERK1/2. *Mol. Cancer Res.* **2023**, *21* (9), 867−880.
(55) Han, Z.; Zhang, Y.; Sun, Y.; Chen, J.; Chang, C.; Wang, X.; Yeh, S. ERβ-Mediated Alteration of circATP2B1 and miR-204−3p Signaling Promotes Invasion of Clear Cell Renal Cell Carcinoma. *Cancer Res.* **2018**, *78* (10), 2550−2563.
(56) Zhou, Y.; Yin, L.; Li, H.; Liu, L. H.; Xiao, T. The LncRNA LINC00963 facilitates osteosarcoma proliferation and invasion by suppressing miR-204−3p/FN1 axis. *Cancer Biol. Ther.* **2019**, *20* (8), 1141−1148.
(57) Cui, Z. H.; Shen, S. Q.; Chen, Z. B.; Hu, C. Growth inhibition of hepatocellular carcinoma tumor endothelial cells by miR-204−3p and underlying mechanism. *World J. Gastroenterol.* **2014**, *20* (18), 5493−5504.
(58) Jiang, Y.; Liu, Y.; Zhang, Y.; Ouyang, J.; Feng, Y.; Li, S.; Wang, J.; Zhang, C.; Tan, L.; Zhong, J. MicroRNA-142−3P suppresses the progression of papillary thyroid carcinoma by targeting FN1 and inactivating FAK/ERK/PI3K signaling. *Cell. Signalling* **2023**, *109*, 110792.
(59) Zhang, D. L.; Wang, J. M.; Wu, T.; Du, X.; Yan, J.; Du, Z. X.; Wang, H. Q. BAG5 promotes invasion of papillary thyroid cancer cells via upregulation of fibronectin 1 at the translational level. *Biochim. Biophys. Acta, Mol. Cell Res.* **2020**, *1867* (9), 118715.
(60) Wu, T.; Zhang, D. L.; Wang, J. M.; Jiang, J. Y.; Du, X.; Zeng, X. Y.; Du, Z. X. TRIM29 inhibits miR-873−5P biogenesis via CYTOR to upregulate fibronectin 1 and promotes invasion of papillary thyroid cancer cells. *Cell Death Dis.* **2020**, *11* (9), 813.
(61) Mishra, D.; Mishra, A.; Rai, S. N.; Vamanu, E.; Singh, M. P. Identification of Prognostic Biomarkers for Suppressing Tumorigenesis and Metastasis of Hepatocellular Carcinoma through Transcriptome Analysis. *Diagnostics* **2023**, *13* (5), 965.
(62) Mishra, D.; Mishra, A.; Nand Rai, S.; Vamanu, E.; Singh, M. P. Demystifying the Role of Prognostic Biomarkers in Breast Cancer through Integrated Transcriptome and Pathway Enrichment Analyses. *Diagnostics* **2023**, *13* (6), 1142.

https://doi.org/10.1021/acsomega.5c00390
ACS Omega 2025, 10, 19643−19654